A ^{31}P Solid-State Nuclear Magnetic Resonance Study of Phosphate Adsorption at the Boehmite/Aqueous Solution Interface

William F. Bleam*

5626

University of Wisconsin—Madison, Madison, Wisconsin 53706

Philip E. Pfeffer

USDA-ARS Eastern Regional Research Center, Philadelphia, Pennsylvania 19118

Sabine Goldberg

USDA-ARS U.S. Salinity Laboratory, Riverside, California 92502

Robert W. Taylor

Alabama A&M University, Normal, Alabama 35762

Robert Dudley

USDA-ARS Eastern Regional Research Center, Philadelphia, Pennsylvania 19118

Received June 26, 1990. In Final Form: January 31, 1991

Results from ^{31}P solid-state NMR experiments provide direct evidence for the hydrolysis of phosphate molecules adsorbed on the surface of boehmite (γ-AlOOH). Much of the phosphate surface-excess molecules are in chemical environments that are highly sensitive to solution pH, and the phosphate molecules are held relatively immobile. This chemical environment is believed to be inner-sphere surface complexes. The results of "interrupted-decoupling" $^{31}P\{^1H\}$ cross-polarization, magic-angle-spinning NMR experiments are used to discriminate protonated surface phosphate species from those that are fully deprotonated. The pH at which surface phosphates become deprotonated lies somewhere between 9 and 11. This transition pH is an NMR observable which can be predicted by surface-complexation models.

Introduction

The environmental consequence of phosphate pollution occurs mainly in surface waters. Here high levels of bioavailable phosphate, often in concert with high concentrations of dissolved nitrate, stimulate blooms of aquatic vegetation. These blooms deplete dissolved oxygen, killing fish and other aquatic animals. Phosphate bioavailability appears to be controlled through some combination of phosphate-mineral solubility, degradation of organic phosphate compounds, and adsorption at oxide mineral/aqueous solution interfaces.

This study examines phosphate adsorption at the aluminum oxide/aqueous solution interface through modeling and ^{31}P solid-state nuclear magnetic resonance (NMR). Among other things, the surface-complexation model predicts pH-dependent hydrolysis of adsorbed phosphate molecules. The solid-state nuclear magnetic resonance experiments we used monitor hydrolysis of adsorbed phosphate and, if it occurs, precipitation. At issue is whether the picture that emerges from NMR experiments agrees with the representation of the surface-complexation model.

Both precipitation and adsorption can occur when phosphate is added to an aluminum oxide suspension. It is probably impossible to determine where adsorption ends and precipitation begins from measurement of solution ion concentrations alone.[1-7] This transition point defines the adsorbing capacity of the oxide since further increases in the phosphate concentration must include precipitation. We also examine the design of an adsorption experiment that minimizes the likelihood of heterogeneous precipitation while maximizing the amount of phosphate adsorbed.

1. Adsorption Mechanisms. Indirect experimental evidence indicates the principal mechanism of phosphate adsorption on aluminum oxide is ligand exchange resulting in inner-sphere surface complexes. The constant-capacitance model is the simplest surface-complexation model that assumes a ligand-exchange mechanism for specific inner-sphere adsorption of ions at the oxide/aqueous solution interface. This model provides an excellent quantitative description of phosphate adsorption on aluminum and iron oxides.[8] It is expected that more complex surface-complexation models of inner-sphere adsorption, such as the triple-layer model, would also be appropriate.

An advantage of these more complex models is their ability to represent the ionic-strength effects on adsorption. However, inner-sphere adsorption is virtually independent of ionic strength; such is the case for phosphate adsorption on aluminum oxide in NaCl and KCl solutions ranging

(1) Mattson, S.; Alvasaker, E.; Koutler-Andersson, E.; Vahtras, K. *Ann. R. Agric. Coll. Swed.* **1953**, *20*, 19.
(2) Kittrick, J. A.; Jackson, M. L. *J. Soil Sci.* **1957**, *7*, 81.
(3) Hsu, P. H. *Soil Sci. Soc. Am. Proc.* **1964**, *28*, 474.
(4) Hsu, P. H. *Soil Sci.* **1965**, *99*, 398.
(5) Veith, J. A.; Sposito, G. *Soil Sci. Soc. Am. J.* **1977**, *41*, 697.
(6) van Riemsdijk, W. H.; Lyklema, J. *Colloids Surf.* **1980**, *1*, 33.
(7) Elprince, A. M.; Sposito, G. *Soil Sci. Soc. Am. J.* **1981**, *45*, 277.
(8) Goldberg, S.; Sposito, G. *Commun. Soil Sci. Plant Anal.* **1985**, *16*, 801.

from 0.002 to 0.2 mol L^{-1}.[9] More complex models were not used in our study because the large increase in the number of adjustable parameters was unnecessary and therefore unacceptable.

Direct spectroscopic evidence of inner-sphere adsorption has proven elusive.[8] The first objective of our study was to investigate the properties of phosphate adsorbed at the boehmite surface by using ^{31}P nuclear magnetic resonance spectroscopy. We designed our experiments to test the following hypothesis: phosphate adsorbed on the surface of boehmite hydrolyzes with varying pH in a manner represented by the constant-capacitance model.[10-12] To test this hypothesis, we combined two approaches: representation of phosphate surface speciation using the constant-capacitance model and execution of NMR experiments designed to discriminate protonated from nonprotonated phosphate species on the oxide surface. Whether adsorbed phosphate forms inner- or outer-sphere surface complexes can be determined from the characteristics of the NMR signals in certain routine experiments.

Our major tool is high-resolution solid-state NMR spectroscopy.[13-16] Direct measurements of ^{1}H–^{31}P nuclear magnetic dipole interactions employ variations of the cross-polarization (CP) experiment of Pines et al.[17] For instance, Rothwell et al.[18] and Tropp et al.[19] made qualitative comparisons of CP magic-angle-spinning (CP-MAS) and single-pulse-excitation, magic-angle-spinning (MAS) spectra. The ^{31}P resonances more strongly "coupled" to ^{1}H nuclei show a signal enhancement in CP-MAS spectra relative to MAS spectra. Aue and co-workers[20,21] expanded this approach by including "dipole suppression", also known as "interrupted-decoupling",[22] CP-MAS experiments. The ^{31}P resonances more strongly "coupled" to ^{1}H show a suppression in the "interrupted-decoupling" CP-MAS spectra relative to MAS spectra.

2. Boehmite Adsorption Capacity. Measuring the phosphate adsorption maximum on an oxide mineral surface was another objective of this study. Phosphate is one of many molecules capable of both adsorbing at a mineral interface and forming a mineral with components of the adsorbent. Unfortunately, the transition from adsorption to precipitation is ill-defined with the consequence that the adsorption capacity itself is ambiguous.

We believe that a means for resolving this dilemma is embodied in the observation by Hsu and Rennie[23] as they wrote of phosphate adsorption on aluminum oxides: "the adsorption capacity at various pH values can be compared only when all solutions are saturated with aluminum phosphate". Referring to this as the Hsu–Rennie condition, we believe it is a prescription for measuring maximum adsorbate surface excess that is tied to mineral solubilities and solution speciation. It stands in contrast to the Langmuir method for determining the phosphate adsorption maximum.[24] Though the Langmuir equation has a mathematical form suitable for modeling adsorption isotherms (viz., the function approaches a limiting value asymptotically), the validity of physical interpretations assigned to the parameters has been strongly questioned.[5]

Application of the Hsu–Rennie condition is most practically achieved by using the "concentration-null" method for measuring adsorbate surface excess. In the "concentration-null" method, one determines the amount of the adsorbed component which has to be added to return the solution to the original composition.[25] In our case this original solution composition is determined by mineral solubilities. Because we are adsorbing phosphate on the surface of boehmite (γ-AlOOH), the original solution compositions in our pH-dependent phosphate adsorption experiment are in solubility equilibrium with boehmite. The phosphate concentrations in the original solutions depend on the solubility of the aluminum phosphate likely to form in these suspensions. The Hsu–Rennie condition is satisfied when at slight aluminum phosphate undersaturation, repeated additions of phosphate yield no further decrease in the solution phosphate concentration.

Materials

We prepared synthetic boehmite by using the following modification of the procedure reported by Santos et al.[26] This was done by weighing 4.25 g of Al metal powder into a 1-L Erlenmeyer flask, adding 200 mL of 0.5 mmol L^{-1} $HgCl_2$ solution, and stirring for 10 min. This allowed a surface amalgam to form which eliminates oxide impurities on the surface of the metal that could nucleate phases other than boehmite.

The metal powder was washed thoroughly with distilled, deionized water, then 12.5 mL of glacial acetic acid and 50 mL of distilled, deionized water were added. The mixture was stirred while heated at 75 °C until H_2 gas evolved and allowed to stand at room temperature overnight.

Boiling at constant volume (maintaining volume with distilled, deionized water) for about 8 h drove off excess acetic acid and allowed crystal nuclei to form. The reaction preparation was then heated in a pressure vessel at 170 °C for 8 h to form the boehmite. There will still be some acetate adsorbed to the boehmite and we removed this by freeze-drying the colloidal suspension and then resuspending the boehmite in 250 mL of 30% H_2O_2. This suspension was boiled at constant volume for 6 h (maintaining volume with distilled, deionized water) to remove all traces of acetate. Finally, the colloidal boehmite suspension was freeze-dried for storage. The aluminum metal was a 99.99% purity, 100 mesh powder from Aldrich Chemical Co., Inc.; all other chemicals were reagent grade.

We prepared several boehmite batches, combining them at the end of the synthesis. The specific surface area was 187.2 m^2/g, determined by Porous Products, Ithaca, NY, using the standard multipoint BET procedure (N_2 was the adsorbing gas). Scanning electrode microscopy revealed that the boehmite crystals were fibers 0.4–0.6 μm in length and about 0.05 μm in diameter. Results of powder X-ray diffraction analysis using Cu Kα radiation (λ = 1.5405 Å) are shown in Table I (cf. PDF 7-324,

(9) Helyar, K. R.; Munns, D. N.; Burau, R. G. *J. Soil Sci.* **1976**, *27*, 307.
(10) Hohl, H.; Sigg, L.; Stumm, W. In *Particulates in Water*; Kavanaugh, M. C., Leckie, J. O., Eds.; Advances in Chemistry Series 189; American Chemical Society: Washington, DC, 1980; p 1.
(11) Stumm, W.; Kummert, R.; Sigg, L. *Croat. Chem. ACta*, **1980**, *53*, 291.
(12) Sigg, L.; Stumm, W. *Colloids Surf.* **1981**, *2*, 101.
(13) Andrew, E. R. *Int. Rev. Phys. Chem.* **1981**, *1*, 195.
(14) Fyfe, C. A.; Bemi, L.; Clark, H. C.; Curtin, D.; Davies, J.; Drexler, D.; Dudley, R. L.; Gobbi, G. C.; Hartmen, J. S.; Klinowski, J.; Hayes, P.; Lenkinski, R. E.; Lock, C. J. L.; Paul, I. C.; Rudin, A.; Tchir, W.; Thomas, J. M.; Wasylishen, F. R. S.; Wasylishen, R. E. *Philos. Trans. R. Soc., A* **1982**, *305*, 591.
(15) Fyfe, C. A.; Bemi, L.; Clark, H. C.; Davies, J. A.; Gobbi, G. C.; Hartmen, J. S.; Hayes, P. J.; Wasylishen, R. E. In *Inorganic Chemistry: Toward the 21st Century*; Chisholm, M. H., Ed.; American Chemical Society: Washington, DC, 1983; p 405.
(16) Kirkpatrick, R. J.; Smith, K. A.; Schramm, S.; Turner, G.; Yang, W.-H. *Annu. Rev. Earth Planet. Sci.* **1985**, *13*, 29.
(17) Pines, A.; Gibby, M. G.; Waugh, J. S. *J. Chem. Phys.* **1973**, *59*, 569.
(18) Rothwell, W. P.; Waugh, J. S.; Yesinowski, J. P. *J. Am. Chem. Soc.* **1980**, *102*, 2637.
(19) Tropp, J.; Blumenthal, N. C.; Waugh, J. S. *J. Am. Chem. Soc.* **1983**, *105*, 22.
(20) Aue, W. P.; Roufosse, A. H.; Glimcher, M. J.; Griffin, R. G. *Biochemistry* **1984**, *23*, 6110.
(21) Roufosse, A. H.; Aue, W. P.; Roberts, J. E.; Glimche, M. J.; Griffin, R. G. *Biochemistry* **1984**, *23*, 6115.
(22) Opella, S. J.; Frey, M. H. *J. Am. Chem. Soc.* **1979**, *101*, 5854.
(23) Hsu, P. H.; Rennie, D. A. *Can. J. Soil Sci.* **1962**, *42*, 197.
(24) Olsen, S. R.; Watanabe, F. S. *Soil Sci. Soc. Am. Proc.* **1957**, *21*, 144.
(25) Nunn, C. C.; Evertt, D. H. *J. Chem. Soc., Faraday Trans. 1* **1983**, *79*, 2953.
(26) Santos, P. S.; Santos, H. S.; Neves, R. F. 1985, 8th International Clay Conference, Denver, CO, 1985.

Table I. Powder X-ray Diffraction Data for Synthetic Boehmite, Spacings [d] in Angstroms

synthetic boehmite		boehmite[a]	
d	I	d	I
6.17	100	6.11	100
3.18	71	3.164	65
2.36	55	2.346	55
1.99	4	1.980	6
1.86	42	1.860	30
1.85	42	1.850	25
1.78	4	1.770	6
1.66	24	1.662	14
1.53	13	1.527	6
1.45	26	1.453	16
		1.434	10
		1.412	2
		1.396	2
1.39	13	1.383	6
		1.369	2
1.31	39	1.312	16

[a] Powder Diffraction File No. 21-1307.

PDF 20-11, PDF 5-355, and PDF 10-173). No effort was made to determine whether poorly crystalline phases were present.

Experimental Methods

1. Preparation of Suspensions and Measurement of Proton Surface Charge. We used stock suspensions containing 6250 m^2 of boehmite L^{-1} to prepare 1000 m^2 L^{-1} suspensions for proton surface charge measurement and 250 m^2 L^{-1} suspensions for both microelectrophoresis and the phosphate-adsorption experiments. All suspensions contained 0.001 mol L^{-1} KCl as a background electrolyte, the pH being adjusted by tenth molar standardized solutions of either KOH or HCl. We used KH_2PO_4 (KDP) as our source of phosphate and $AlCl_3$ as the source of aluminum. All suspensions were prepared with CO_2-free distilled, deionized water and stored in polyethylene bottles under N_2 gas.

2. Analytical Techniques. To measure proton surface charge, we prepared 25 mL of a 1000 m^2 L^{-1} suspension, adjusted the suspension to pH = 3, and titrated the suspension, in 0.25 pH unit steps, up to pH = 11. We used a tenth molar standardized KOH solution for the titration. This was repeated by adjusting the pH of the suspension to 11 with KOH followed by incremental titration to pH 3 using a standardized tenth molar HCl solution. At each increment, the pH was maintained until the rate of change is less than 0.01 pH unit per minute.

The proton surface charge experiment employed a Radiometer System ETS822 autotitratator. We used a Corning Model-150 pH/Ion meter for pH measurements in all other experiments. Microelectrophoresis measurements were taken with a Pen Kem Model-501 Lazer Zee Meter. We analyzed total phosphate and total aluminum spectrophotometrically, using the Murphy–Riley method[27] for phosphate analysis and the method of Bloom et al.[28] for aluminum.

Solution proton-decoupled ^{31}P NMR spectra were obtained on a JEOL JNM-GX-400 spectrometer operating at 9.4 T (viz., 161.9 MHz ^{31}P resonance frequency). Proton-decoupled ^{31}P spectra were obtained on a Bruker MSL-300 NMR spectrometer operating at 7.0 T (viz., ^{31}P resonance frequency of 121.49 MHz). The 90° pulse width for the JNM-GX-400 spectrometer was 22 μs for ^{31}P. The 90° pulse width for the MSL-300 spectrometer was 5 μs for both ^1H and ^{31}P and spinning frequencies were approximately 3 kHz.

3. Adsorption Experiments. All suspensions in our adsorption experiments contained 250 m^2 of boehmite per liter. We used values for the equilibrium ion activity products for the boehmite solubility and the hydrolysis of aluminum and orthophosphate ions from Lindsay.[29] Lindsay does not list activity products for the formation of aluminum–phosphate solution complexes, yet there is abundant evidence for such species.[30-35] We estimated their formation by using constants listed by Novozamsky and Beek.[36] Finally, we chose to use amorphous aluminum phosphate as the phase determining the upper limit on phosphate solubility. Our calculations employed the activity product for amorphous aluminum phosphate reported by Veith and Sposito.[37] Minimum phosphate solubility, corresponding to a total solution phosphate concentration of about 0.4 mmol L^{-1}, occurs at pH ≈4.5 in such a system.

We chose to use a solution concentration of 0.1 mmol L^{-1} throughout the pH range of 3–11 because preliminary experiments showed that the adsorption capacity of our boehmite suspensions above pH = 5 and below pH = 4 was too low to reliably measure significant concentration changes in solutions containing 1 mmol L^{-1} phosphate and above. The solubility and amorphous aluminum phosphate rapidly exceeds that concentration above and below the pH of minimum solubility.

To perform the phosphate adsorption experiment we began by preparing replicate 250 m^2 L^{-1} boehmite suspensions. We adjusted the pH of each suspension to the desired value and immediately added sufficient $AlCl_3$ solution to bring the suspension into solubility equilibrium, continuing to adjust the pH until stable. We used a Radiometer System ETS822 autotitratator to maintain pH-stat. After 24 h, we readjusted the pH when necessary and added sufficient KDP solution to yield an initial total phosphate concentration of 0.1 mmol L^{-1} and maintained the pH at the chosen value. After 24 h, we measured the pH of one set of replicate suspensions (we performed at least three replicates for each treatment), centrifuged each suspension at 15 000 rpm on a Sorvall centrifuge for 20 min, filtered the supernatant through a membrane filter (Nuclepore Corp., polycarbonate, 0.2 μm pore diameter), and analyzed for total soluble phosphate.

If the soluble phosphate concentration after adsorption was lower than 0.1 mmol L^{-1}, we added KDP to return the phosphate concentration to 0.1 mmol L^{-1} in the remaining sets of replicates, adjusting the solution pH if necessary. Sampling of a second set of replicates followed this second addition by 24 h (adsorption kinetic studies showed that the phosphate concentration in solution did not change after a period of 3 h following the addition of KDP to the suspension). If the soluble phosphate concentration was, once again, lower than the initial 0.1 mmol L^{-1} concentration, we added KDP to return the phosphate concentration to 0.1 mmol L^{-1} in the remaining set of replicates and took samples as just described 24 h later.

The "concentration null" method requires that the initial and the final phosphate concentration be equal. The boehmite suspensions were undersaturated with respect to amorphous aluminum phosphate. Near the pH of maximum adsorption, we had to make three additions to KDP before the adsorbing capacity of the boehmite was saturated. Two additions were sufficient when the adsorption maximum fell below ≈1 μmol m^{-2}.

For ^{31}P solid-state NMR analysis, we prepared suspensions and performed adsorption experiments as described above. We reserved the solids after the final step and freeze-dried them. We prepared suspensions for microelectrophoresis in the same way that we prepared them for adsorption experiments. The "pristine" samples, of course, did not receive any KDP. Because light scattering was too great in dispersed suspensions to measure mobilities, we centrifuged for 20 min at 15 000 rpm and resuspended a small fraction of the boehmite in the supernatant solution before measuring the zeta potential.

(27) Murphy, J.; Riley, J. P. *Anal. Chim. Acta* 1962, *27*, 31.
(28) Bloom, P. R.; Weaver, R. M.; McBride, M. B. *Soil Sci. Soc. Am. J.* 1978, *42*, 713.
(29) Lindsay, W. L. *Chemical Equilibria in Soils*; Wiley: New York, 1979.
(30) Jameson, R. F.; Salmon, J. E. *J. Chem. Soc.* 1954, 4013.
(31) Salmon, J. E.; Wall, J. G. L. *J. Chem. Soc.* 1958, 1128.
(32) Akitt, J. W.; Greenwood, N. N.; Lester, G. D. *J. Chem. Soc. A* 1971, 2450.
(33) Karlik, S. J.; Elgavish, G. A.; Pillai, R. P.; Eichhorn, G. L. 1982, *J. Magn. Reson.* 1982, *49*, 164.
(34) Karlik, S. J.; Elgavish, G. A.; Pillai, R. P.; Eichhorn, G. L. *J. Am. Chem. Soc.* 1983, *105*, 602.
(35) Wilson, M. A.; Collins, P. J.; Akitt, J. W. *Anal. Chem.* 1989, *61*, 1253.
(36) Novozamsky, I.; J. Beek In *Soil Chemistry Part A: Basic Elements*; Bolt, G. H., Bruggenwert, M. G. M., Eds.; Elsevier: New York, 1976; p 96.
(37) Veith, J. A.; Sposito, G. *Soil Sci. Soc. Am. J.* 1977, *41*, 870.

4. Constant-Capacitance Model. The constant-capacitance model is a surface-complexation model that assumes a ligand exchange mechanism for specific adsorption of ions at the oxide–solution interface.[13] In the model all surface complexes, including those formed with protons and hydroxyl ions, are inner-sphere complexes located in the same surface plane of adsorption; complex formation with ions from the background electrolyte is not included. The relationship between the surface charge, σ ($mol_c\ L^{-1}$), and the surface potential, ψ (V), is assumed to be linear

$$\sigma = (CSa/F)\psi \quad (1)$$

where C ($C\ V^{-1}\ m^{-2}$) is the capacitance density parameter, S ($m^2\ g^{-1}$) is the specific surface area, a ($g\ L^{-1}$) is the suspension density of the solid, and F ($C\ mol_c^{-1}$) is the Faraday constant.

In the application of the model to phosphate adsorption on boehmite, the following surface reactions are defined:

$$\equiv AlOH^0_{(s)} + H^+_{(aq)} = \equiv AlOH_2^+{}_{(s)} \quad (2)$$

$$\equiv AlOH^0_{(s)} = \equiv AlO^-_{(s)} + H^+_{(aq)} \quad (3)$$

$$\equiv AlOH^0_{(s)} + H_3PO_{4(aq)} = \equiv AlH_{(2-x)}PO_4^{x-}{}_{(s)} + H_2O + xH^+_{(aq)} \quad (4)$$

where $x-$ is the charge on the phosphate surface complex (x = 0, 1, or 2) and $\equiv AlOH^0_{(s)}$ represents 1 mol of reactive surface hydroxyls bound to an Al^{3+} ion at the boehmite interface.

The above reactions are described by the following intrinsic conditional equilibrium constants:

$$K_{+(int)} = \exp(\psi F/RT)[\equiv AlOH_2^+]/([\equiv AlOH^0][H^+]) \quad (5)$$

$$K_{-(int)} = \exp(-\psi F/RT)([\equiv AlO^-][H^+])/[\equiv AlOH^0] \quad (6)$$

$$K_{P\ (int)}^{\ i} = \exp(-x\psi F/RT)([\equiv AlH_{(2-x)}PO_4^{x-}][H^+]^x)/([\equiv AlOH^0][H_3PO_4]) \quad (7)$$

where $i = x + 1$, R is the molar gas constant, and T is the absolute temperature and brackets represent concentrations ($mol\ L^{-1}$).

Intrinsic conditional equilibrium constants are obtained by extrapolation of ordinary conditional equilibrium constants to zero net surface charge.[13] Conditional equilibrium constants for adsorbed phosphate take the form

$${}^cK_P^{\ i} = ([\equiv AlH_{(2-x)}PO_4^{x-}][H^+]^x)/([\equiv AlOH^0][H_3PO_4]) \quad (8)$$

The mass balance equation for the surface functional group, $\equiv AlOH$, is

$$[\equiv AlOH]_T = [\equiv AlOH^0] + [\equiv AlOH_2^+] + [\equiv AlO^-] + [\equiv AlH_2PO_4^0] + [\equiv AlHPO_4^-] + [\equiv AlPO_4^{2-}] \quad (9)$$

and the charge balance equation is

$$\sigma = [\equiv AlOH_2^+] - [\equiv AlO^-] - [\equiv AlHPO_4^-] - 2\,[\equiv AlPO_4^{2-}] \quad (10)$$

The above set of equations defines the equilibrium problem for phosphate adsorption on the aluminum oxide.

The computer program FITEQL[38] was used to obtain the values of the intrinsic surface protonation–dissociation constants, log $K_{\pm(int)}$, and the intrinsic surface complexation constants, log $K_{P^i(int)}$. FITEQL contains the constant-capacitance model and used a nonlinear least-squares optimization technique to fit equilibrium constants to experimental adsorption data. Values of the intrinsic protonation–dissociation constants can be calculated from potentiometric titration curves of proton surface charge. In this analysis,[13] it is assumed that the net surface charge, σ, is equal to $[\equiv AlOH_2^+]$ at pH values below the *point of zero net proton charge* (PZNPC) and is equal to $-[\equiv AlO^-]$ at pH values above PZNPC.

The intrinsic conditional protonation–dissociation constants are related to the conditional protonation–dissociation constants

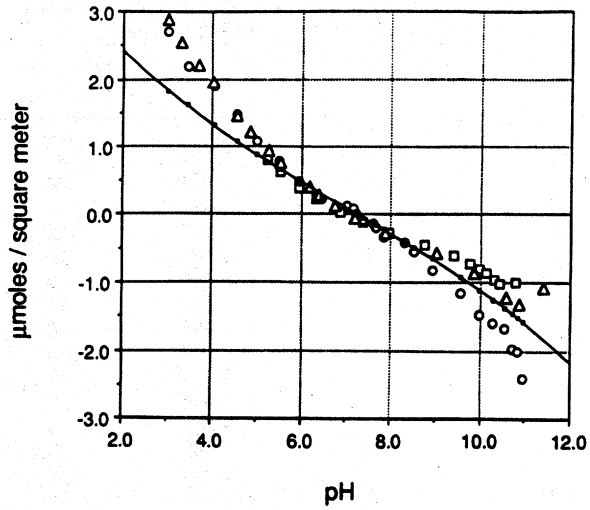

Figure 1. Proton surface charge of boehmite (γ-AlOOH). Aqueous suspensions contain 1000 $m^2\ L^{-1}$ boehmite (187.2 $m^2\ g1^{-1}$) and 0.001 $mol\ L^{-1}$ KCl. Open symbols indicate experimental data (three experiments: circles, triangles, and squares), while the smooth curve is the fit by the constant capacitance model to the combined titration data.

as follows:

$$K_{\pm(int)} = {}^cK_\pm \exp(\pm\psi F/RT) \quad (11)$$

After converting surface charge, σ, to surface potential, ψ, using eq 1 and transforming both sides to common logarithms, the equation can be solved for log ${}^cK_\pm$

$$\log {}^cK_\pm = \log K_{\pm(int)} \pm \sigma F^2/\ln(10)\ CSaRT \quad (12)$$

By plotting log ${}^cK_\pm$ versus σ, log $K_{\pm(int)}$ is obtained from the y intercept and the capacitance density parameter, C, can be extracted from the slope. The PZNPC, defined in the constant capacitance model as

$$PZNPC = (\log K_{+(int)} - \log K_{-(int)})/2 \quad (13)$$

can subsequently be obtained.

Experimental Results

1. Surface-Charge Properties. The PZNPC for the pristine boehmite is about 7.2 (Figure 1), lower than that reported for other aluminum oxides.[39–42] The point of zero charge (PZC) for the pristine boehmite is about 9.4 (Figure 2), in close agreement with PZCs for boehmite and other aluminum oxides reported elsewhere.[39,40,43–46] Proton surface charge was measured by using the conventional titration technique; no provision was made to bring the boehmite suspension into solubility equilibrium during the course of the titration experiment. The suspensions used in the microelectrophoresis experiments, on the other hand, were brought into solubility equilibrium through the addition of $AlCl_3$ prior to the mobility measurements.

Adsorption of phosphate dramatically changes the zeta potential of the boehmite (Figure 2), lowering it from 9.4 to about 5.7. The effect of phosphate adsorption, as with

(38) Westall, J. FITEQL: A program for the determination of chemical equilibrium constants from experimental data; Report No. 82-01; Department of Chemistry, Oregon State University: Corvallis, OR, 1982.

(39) Yoppa, J. A.; Fuerstenau, D. W. *J. Colloid Sci.* **1964**, *19*, 61.
(40) Sadek, H.; Helmy, A. K.; Sabet, V. M.; Tadros, T. F. *J. Electroanal. Chem.* **1970**, *27*, 257.
(41) Wiese, G. R.; Healy, T. W. *J. Colloid Interface Sci.* **1975**, *51*, 427.
(42) Matijevic, E. *Pure Appl. Chem.* **1978**, *50*, 1193.
(43) Parks, G. A. *Chem. Rev.* **1965**, *65*, 177.
(44) Alwitt, R. S. *J. Colloid Interface Sci.* **1972**, *40*, 195.
(45) Brace, R.; Matijevic, E. *J. Inorg. Nucl. Chem.* **1974**, *35*, 3691.
(46) Anderson, M. A.; Malotky, D. T. *J. Colloid Interface Sci.* **1979**, *72*, 413.

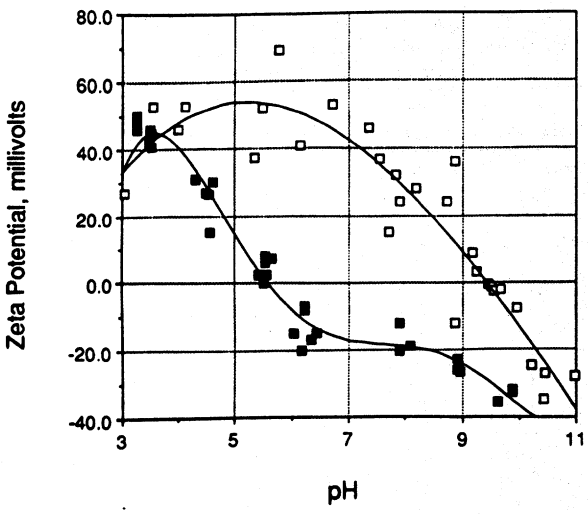

Figure 2. Zeta potential of pristine and phosphate-containing boehmite (γ-AlOOH) suspensions. Aqueous suspensions contain 250 $m^2 L^{-1}$ boehmite (187.2 $m^2 g^{-1}$) and 0.001 mol L^{-1} KCl. Open squares indicate pristine suspensions; filled squares indicate phosphate-containing suspensions. The final phosphate concentration in all phosphate-containing suspensions was 0.1 mmol L^{-1}, added as potassium dihydrogen phosphate.

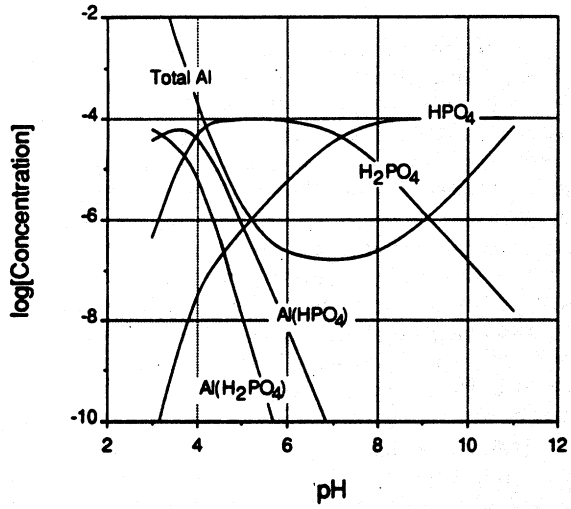

Figure 3. Solution phosphate speciation in aqueous boehmite (γ-AlOOH) suspensions. Total phosphate concentration equals 0.1 mmol L^{-1}.

other second-period oxyanions,[12,13,44,46-49] is to reduce the magnitude of the positive charge on the surface. This effect is well-known and has led some to suggest that this occurs through the direct displacement by phosphate ligands of aquo and hydroxo ligands coordinating surface metal cations.[46,40-52]

Values for the intrinsic conditional protonation–dissociation constants and the capacitance density parameter were obtained by plotting the potentiometric titration data in the form of eq 5. The total number of reactive sites, $[\equiv AlOH]_T$, was set equal to 2.87 mmol L^{-1} (equivalent to 2.87 μmol m^{-2} or ≈57.9 $Å^2$ per site), the largest value of $[\equiv AlOH_2^+]$ occurring at pH = 3. Each titration curve was analyzed separately and the resulting $\log K_{\pm(int)}$ and C values were averaged: $\log K_{+(int)} = 5.6 \pm 0.2$, $\log K_{-(int)} = -8.6 \pm 0.2$, and $C = 1.8 \pm 0.9$. The PZNPC obtained by using eq 13 is equal to 7.1 and compares well with the crossover point at pH = 7.2 in Figure 1. Values for the intrinsic conditional protonation–dissociation constants were also obtained by fitting the potentiometric titration data with the FITEQL program. Because of the large standard deviation in the value of the experimental capacitance density, C was set equal to 1.06 C V^{-1} m^{-2}, a value used in a previous application of the constant-capacitance model to phosphate adsorption on aluminum oxide minerals.[54] All titration data were analyzed by FITEQL simultaneously. The resulting constants are $\log K_{+(int)} = 6.02$ and $\log K_{-(int)} = -8.45$. The PZNPC obtained by FITEQL of 7.24 is virtually identical with the crossover point of 7.2 and agrees well with the linear extrapolation value of 7.1. The fit of the constant-capacitance model to the potentiometric titration data is excellent and is shown in Figure 1.

2. Phosphate Adsorption Envelope. Figure 3 shows the activities of the major solution–phosphate species as predicted by using the activity constants mentioned above. The system consists of boehmite suspensions containing 250 m^2 L^{-1} with an ionic strength of 0.001 and a total phosphate concentration of 0.1 mmol L^{-1}. The total concentration of aluminum is not, of course, constant since it follows the solubility of the boehmite. Aluminum–phosphate solution complexes are the dominant phosphate solution species at and below pH ≈ 4.

The actual adsorption envelope, measured by using the concentration-null method, is shown in Figure 4. Two characteristics of this adsorption envelope warrant comment. First, and most obvious, the adsorption envelope is sharply peaked at pH ≈ 4, declining rapidly in the pH range 4 to 3. This form of adsorption envelope has been observed by both Chen et al. and Huang,[53,55] the adsorption maxima occurring at about the same pH in their studies as found in ours. Muljadi et al.[56] report adsorption data for both gibbsite and pseudoboehmite, which do not show an adsorption maximum at pH ≈ 4. This phosphate adsorption behavior[53,55] is in contrast to that commonly observed for goethite, for which the adsorption capacity continues to increase below pH = 4.[14,48,49,57-59]

The second characteristic is that the pH of maximum phosphate adsorption we found is somewhat lower than that reported for other aluminum oxides.[46,53,55] Notice that the overall shape in the adsorption envelope (Figure 4) is similar to the trend in the concentration of $AlHPO_4^+{}_{(aq)}$ (Figure 3).

It is interesting to compare our results with those of Anderson and Malotky.[46] They reported a lowering of the PZC from 9.3 (pristine γ-Al_2O_3) to 5.6 (phosphate-"saturated" γ-Al_2O_3). Their PZC = 5.6 was determined at $\Gamma_{max}^{Phosphate}$ and compares with our measured PZC ≈ 5.7, also at $\Gamma_{max}^{Phosphate}$ (Figure 2). Their estimate of $\Gamma_{max}^{Phosphate}$, measured by using adsorption isotherms, was 2.1 μmol m^{-2} compared to our estimate, with 95% confidence interval, of 1.8 ± 0.3 μmol m^{-2} (Figure 4).

(47) Hingston, F. J.; Atkinson, R. J.; Posner, A. M.; Quirk, J. P. *Nature* **1967**, *215*, 1459.
(48) Bowden, J. W.; Nagarajah, S.; Barrow, N. J.; Posner A. M.; Quirk, J. P. *Aust. J. Soil Res.* **1980**, *18*, 49.
(49) Barrow, N. J.; Bowden, J. W. *J. Colloid Interface Sci.* **1987**, *119*, 236.
(50) Rajan, S. S. S.; Perrott, K. W.; Saunders, W. M. H. *J. Soil Sci.* **1974**, *25*, 438.
(51) Rajan, S. S. S. *Nature* **1976**, *262*, 45.
(52) McLaughlin, J. R.; Ryden, J. C.; Syers, J. K. *J. Soil Sci.* **1981**, *32*, 365.
(53) Chen, Y.-S.; Butler, J. N.; Stumm, W. *J. Colloid Interface Sci.* **1973**, *43*, 421.
(54) Goldberg, S.; Sposito, G. *Soil Sci. Soc. Am. J.* **1984**, *48*, 772.
(55) Huang, C. P. *J. Colloid Interface Sci.* **1975**, *53*, 178.
(56) Muljadi, D.; Posner, A. M.; Quirk, J. P. *J. Soil Sci.* **1966**, *17*, 212.
(57) Hingston, F. J.; Atkinson, R. J.; Posner, A. M.; Quirk, J. P. *Trans. 9th Int. Cong. Soil Sci.* **1968**, *1*, 669.
(58) Hingston, F. J.; Posner, A. M.; Quirk, J. P. *J. Soil Sci.* **1972**, *23*, 177.
(59) Barrow, N. J.; Bowden, J. W.; Posner, A. M.; Quirk, J. P. *Aust. J. Soil Res.* **1980**, *18*, 395.

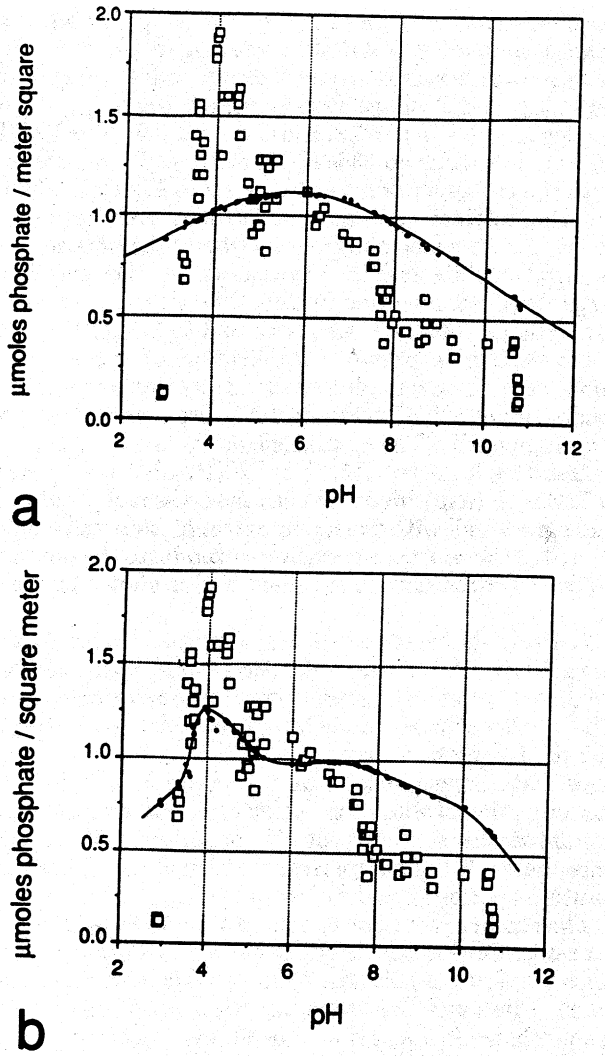

Figure 4. Phosphate surface excess at the interface between aqueous solution and boehmite (γ-AlOOH) as a function of pH. Aqueous suspensions contain 0.1 mmol L^{-1} phosphate, 250 m^2 L^{-1} boehmite (187.2 m^2 g^{-1}), and 0.001 mol L^{-1} KCl. Phosphate surface excess was measured by the concentration-null method. The smooth curves are the fit by the constant capacitance model to the experimental data: (a) without aluminum phosphate solution complexes; (b) with aluminum phosphate solution complexes.

Clearly, the results we measured agree well with those observed by others.

The constant-capacitance model was used to describe the experimental phosphate-adsorption data on boehmite. Previous applications of the model to phosphate adsorption on aluminum oxides[54] have not included aluminum–phosphate solution complexes. The ability of the constant-capacitance model to describe phosphate adsorption was tested with and without the consideration of these species. The stoichiometry of the equilibrium problem defined for the model application including aluminum phosphate solution complexes is provided in Table II. The total number of reactive sites, $[\equiv AlOH]_T$, was set equal to 0.478 mmol L^{-1} (equivalent to 1.91 μmol m^{-2} or ≈86.9 Å^2 per site), the maximum phosphate surface excess at pH = 4. The intrinsic conditional protonation–dissociation constants were set to the values obtained from linear extrapolation of the potentiometric titration data and C was set equal to 1.06 C V^{-1} m^{-2}.

In the initial analysis, the three phosphate surface complexation constants, log $K_{P^i(int)}$, were optimized by the FITEQL program. This preliminary calculation indicated that log $K_{P^2(int)}$, the phosphate surface constant for the formation of $\equiv AlHPO_4^-{}_{(s)}$, was unnecessary. Subsequently only two phosphate surface constants were optimized by the FITEQL program. The ability of the constant-capacitance model to describe phosphate adsorption on boehmite is indicated in Figure 4. The model underestimates adsorption at low pH and overestimates it at high pH. Interestingly, without consideration of aluminum phosphate solution complexes, the model results indicate no peak in the surface excess at pH = 4 (Figure 4a). Upon inclusion of these species, the model results describe an adsorption envelope that, like the experimental data, peaks sharply at pH = 4 (Figure 4b). These results suggest that the observed decrease in phosphate adsorption at low pH need not be due to the minimum solubility of aluminum oxide as postulated by Chen et al.[53] but simply occurs because solution phosphate concentrations are reduced by forming an aluminum–phosphate complex that does not adsorb.

Table II. Stoichiometry of the Equilibrium Problem: Phosphate Adsorbed at the Interface between Aqueous Solution and Boehmite (γ-AlOOH)

species	≡Al-OH(s)	$de^{-\psi F/RT}$	K^+	Al^{3+}	H_3-PO_4	H^+	log $K_{(int)}$
H^+(aq)	0	0	0	0	0	1	0.00
OH^-(aq)	0	0	0	0	0	−1	−14.00
$\equiv AlOH^0$(s)	1	0	0	0	0	0	0.00
K^+(aq)	0	0	1	0	0	0	0.00
Al^{3+}(aq)	0	0	0	1	0	0	0.00
$H_3PO_4^0$(aq)	0	0	0	0	1	0	0.00
$H_2PO_4^-$(aq)	0	0	0	0	1	−1	−2.15
HPO_4^{2-}(aq)	0	0	0	0	1	−2	−9.35
PO_4^{3-}(aq)	0	0	0	0	1	−3	−21.70
$KH_2PO_4^0$(aq)	0	0	1	0	1	−1	−2.20
$KHPO_4^-$(aq)	0	0	1	0	1	−2	−8.20
KPO_4^{2-}(aq)	0	0	1	0	1	−3	−19.80
$AlOH^{2+}$(aq)	0	0	0	1	0	−1	−5.02
$Al(OH)_2^+$(aq)	0	0	0	1	0	−2	−9.30
$Al(OH)_3^0$(aq)	0	0	0	1	0	−3	−14.99
$Al(OH)_4^-$(aq)	0	0	0	1	0	−4	−23.33
$Al_2(OH)_2^{4+}$(aq)	0	0	0	2	0	−2	−7.69
$AlH_2PO_4^{2+}$(aq)	0	0	0	1	1	−1	1.00
$AlHPO_4^+$(aq)	0	0	0	1	1	−2	−1.90
$\equiv AlOH_2^+$(s)	1	1	0	0	0	1	5.60
AlO^-	1	−1	0	0	0	−1	−8.63
$\equiv AlH_2PO_4^0$(s)	1	0	0	0	1	0	7.28
$\equiv AlPO_4^{2-}$(s)	1	−2	0	0	1	−2	−1.05

3. ^{31}P Nuclear Magnetic Resonance Spectroscopy of Surface-Adsorbed Phosphate. The ^{31}P NMR solution spectra of the supernatant solution from a suspension at pH = 3 appears in Figure 5. The resonance signal for uncomplexed solution phosphate should appear at ≈+0.8 ppm, yet the only two resonances appear at ≈−8 and −10 ppm (the resonance at +30.73 ppm is a chemical-shift reference). These two resonances undoubtedly arise from aluminum phosphate solution complexes, though their assignment is uncertain.[32,34,35] More importantly, the phosphate speciation appearing in Figure 3 appears to be qualitatively correct, viz. at low pH values there are negligible amounts of uncomplexes phosphate in our suspensions.

Our solid-state, magic-angle-spinning (MAS) ^{31}P NMR spectra of adsorbed phosphate were collected at five pH values: 4.0, 5.5, 7.0, 9.0, and 11.0. These values include the pH of maximum adsorption (cf. Figure 4) and values corresponding to regions where the constant-capacitance model predicts[54] either a single surface species dominates (4.0 and 11) or two or more species coexist (5.5, 7.0, and 9.0), respectively.

Single-pulse excitation MAS spectra at the pH values mentioned above are shown in Figure 6. There is a single,

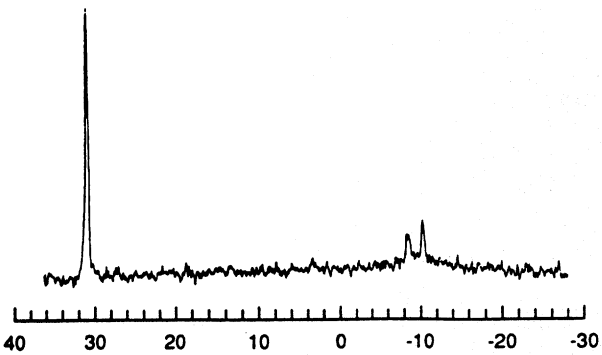

Figure 5. 161.7-MHz ^{31}P single-pulse-excitation, proton-decoupled solution NMR spectra relative to 85% phosphoric acid, scale in ppm. The resonance at 30.73 ppm is from hexamethylphosphoramide which was used as an external chemical shift reference. Supernatant solution is from a phosphate-containing (total phosphate concentration equals 0.1 mmol L^{-1}) aqueous boehmite (γ-AlOOH) suspension at pH = 3.0: 12 μs for a 40° pulse width; 10 000 scans; 2k data points zero-filled to 16k; 16-kHz spectral width; 0.16-s recycle time.

very broad resonance in the pH = 4 spectrum and two signals in the spectra at all other pH values: a narrow, downfield resonance (B_0) and a broad, upfield signal (A_0). There are clearly several unresolved resonances in the A_0 peak. The spectra at pH = 5.5 and pH = 7.0 are quite similar to one another, as are the spectra at pH = 9.0 and pH = 11.0 similar to each other.

It appears that at a third "peak" is present in Figure 6b,c at ≈20 ppm and in Figure 6e a shoulder at ≈−5 ppm. The signal-to-noise ratio of the ≈20 ppm "peak" (Figures 6b,c) is very low and we cannot be certain that it truly represents a distinct chemical environment. Although the signal-to-noise ratio of the ≈−5 ppm shoulder in Figure 6e is higher than the ≈20 ppm "peak", none of these represents a significant proportion of the phosphate surface excess. More importantly, there is simply too little signal intensity to make any interpretations about the chemical environments represented by such weak signals.

The pH dependence of the isotropic chemical shifts of the major NMR signals appearing in the spectra of Figure 6 are illustrated in Figure 7. Only the major signals are included in this graph for the reasons just given.

In preparation of Figure 7, it seemed reasonable to connect the downfield B_0 resonances of the 5.5 and 7.0 spectra to one another and to draw a line connecting those in the 9.0 and 11.0 spectra. If we do the same for the upfield A_0 resonances, connecting 5.5 to 7.0 and 9.0 to 11.0, a pattern appears which suggests that the chemical shift of the B_0 resonance varies continuously from ≈0.1 ppm at pH = 5.5 to ≈3.9 ppm at pH = 11.0 and the A_0 resonances vary continuously from ≈−11.2 ppm to ≈1.5 ppm in the same pH range. The pH-dependent ^{31}P chemical shift of solution phosphate is also plotted in Figure 7.

Although the B_0 resonance varies over a chemical-shift range that is about the same as that covered by solution phosphate (0.8 ppm at pH = 4 to 3.4 ppm at pH = 11), clearly the B_0 resonance of adsorbed phosphate and solution phosphate display different pH-dependent chemical-shift behavior. The A_0 resonance covers a much larger chemical-shift range, displaying a great sensitivity to solution pH.

In summary, the pH-dependent chemical shift data of these spectra suggest that the surface-adsorbed phosphate can be grouped into two classes. The chemical shift of one (giving rise to the narrow, downfield B_0 signal) covers a range of ≈3.8 ppm, while the other (the source of the broad, upfield A_0 signal) covers a range of ≈12.7 ppm. The shielding of the A_0 resonance decreases dramatically as the pH increases and it is clearly more sensitive to changes in solution pH. Finally, the broadness and overall appearance of the A_0 resonance strongly suggest that the phosphate species that give rise to this signal reside in a distribution of chemical environments. The range of chemical environments we would associate with the B_0 resonance is much narrower.

Earlier we mentioned a special type of CP-MAS experiment, known as a "dipole suppression" or "interrupted-decoupling" experiment.[23-25] This experiment probes ^1H–^{31}P nuclear-dipole coupling. The results are useful when studying hydrolysis, since it may be possible to use them to discriminate whether or not a phosphate is protonated. In a typical CP-MAS experiment the acquisition of the nuclear magnetic free-induction decay (FID) is initiated ≈1 μs (viz. a 1 μs "delay") following spin-lock and proceeds under conditions of high-power ^1H–^{31}P decoupling. In an "interrupted-decoupling" experiment, the start of FID acquisition, as well as ^1H–^{31}P decoupling, is delayed for some interval of time following spin-lock during which the ^{31}P signal intensity is permitted to decay under the influence of ^1H–^{31}P coupling. The extent of signal loss becomes a measure of ^1H–^{31}P nuclear dipole coupling: the more rapid the signal loss the greater the coupling.

In a previous study,[60] we found that in those phosphate minerals where crystal structure refinements indicate no protonation of the phosphate molecule (e.g., variscite, crandallite, wavellite) the ^{31}P resonance intensity is still ≈20% of its initial value after interrupting ^1H–^{31}P decoupling 250 μs for resonances. The ^{31}P signal intensity is completely lost after the same interrupt interval in those minerals where protonation of the phosphate does occur (e.g., KDP).

^{31}P CP-MAS spectra of surface-adsorbed phosphate are shown in Figures 8–11, two spectra at each pH value. One is a typical CP-MAS spectrum, ≈1 μs delay between the end of spin-lock and the beginning of FID acquisition. Henceforth, we will refer to these simply as CP-MAS spectra. The other is an "interrupted-decoupling" CP-MAS spectrum with a 250-μs delay. We will refer to these as "dephased" CP-MAS spectra. Without exception the A_0 signal is almost completely decayed in the "dephased" CP-MAS spectra while significant signal intensity remains from the B_0 signal. Considering the signal-to-noise level in the "dephased" CP-MAS spectrum at pH = 4.0 (Figure 8), it is difficult to assign signal intensity accurately, yet it is less than 10% of the CP-MAS intensity. For this reason, we interpret this result as evidence that the A_0 resonance arises from a phosphate with protonated oxygens.

There is another point to be made concerning these spectra. First-order spinning side bands (ssb) are quite noticeable in the CP-MAS spectra at every pH for both up- and downfield signals. The ssb of the downfield B_0 signal is more noticeable primarily because the resonance is much narrower than the upfield A_0 signal. The intensity of the ssb in a material free of paramagnetic ions is related to the chemical shift anisotropy of the nuclei associated with that resonance.[60] A rapidly tumbling phosphate molecule would produce a narrow resonance, but it would not have significant ssb intensity since rapid tumbling would tend to average to zero the anisotropic contribution to the chemical shift.

(60) Bleam, W. F.; Pfeffer, P. E.; Frye, J. S. *Phys. Chem. Miner.* **1989**, *16*, 455.

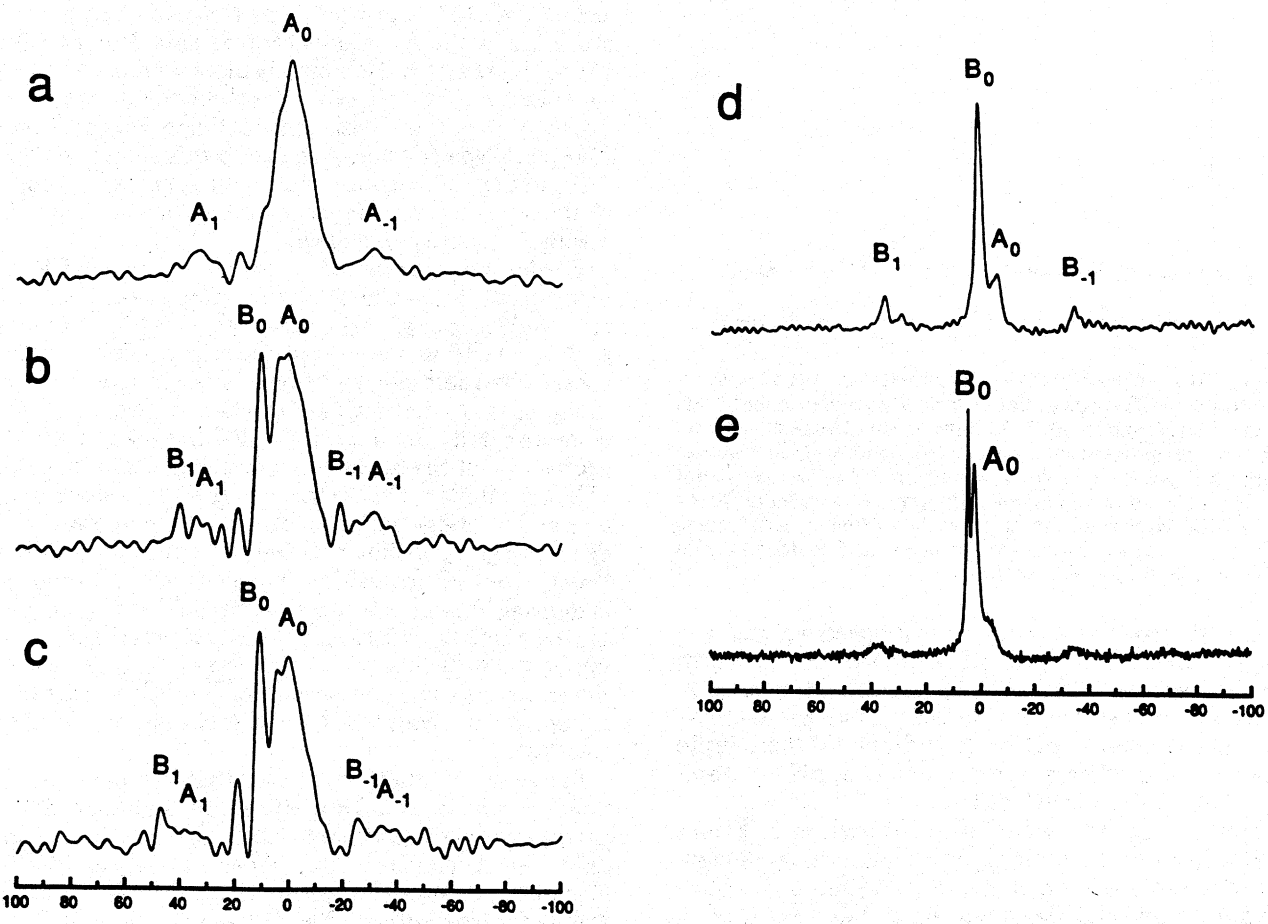

Figure 6. 121.49-MHz ^{31}P single-pulse-excitation solid-state NMR spectra (85% H_3PO_4 external reference, scale in ppm): ≈3 kHz MAS spinning frequency, 256 scans, 35.7 kHz spectral width, 5 s recycle time. Freeze-dried boehmite with surface-adsorbed phosphate: (a) pH = 4.0, 128 data points zero-filled to 8k; (b) pH = 5.5, 128 data points zero-filled to 8k; (c) pH = 7.0, 128 data ponts zero-filled to 8k; (d) pH = 9.0, 256 data points zero-filled to 8k; (e) pH = 11.0, 1k data points zero-filled to 8k. Main peaks are labeled with the subscript "0", first-order spinning sidebands with the subscript "±1".

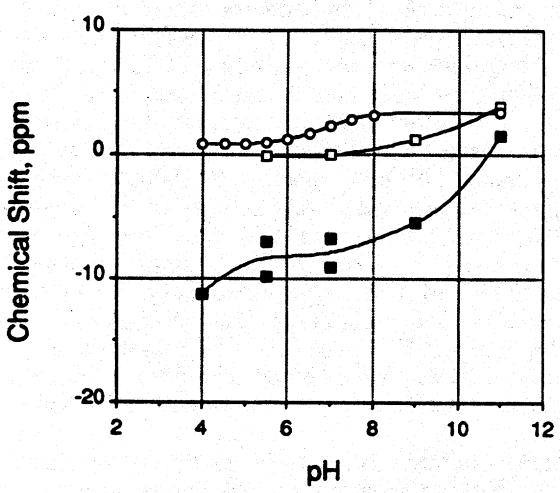

Figure 7. ^{31}P chemical shift as a function of pH. Squares indicate the single-pulse-excitation chemical shift data for phosphate adsorbed on the surface of boehmite (cf. Figure 6). Filled squares correspond to the peaks labeled "A_0" while open squares indicate the "B_0" resonance. Circles indicate the chemical shift NMR data for 0.1 mmol L^{-1} potassium phosphate solutions.

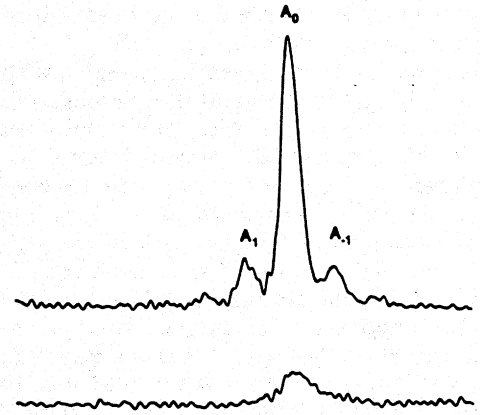

Figure 8. 121.49-MHz ^{31}P cross-polarization solid-state NMR spectra (85% H_3PO_4 external reference, scale in ppm): 256 scans; 128 data points zero-filled to 8k; 35.7-kHz spectral width; 5-s recycle time; 600-μs contact time. Freeze-dried boehmite with surface-adsorbed phosphate from a pH = 4.0 suspension, delay between spin-lock and acquisition: 1 μs (upper); 250 μs (lower). Main peaks are labeled with the subscript "0", first-order spinning sidebands with the subscript "±1".

We estimated the relative intensities of the up- and downfield signals by determining the relative peak areas from single-pulse MAS spectra (Figure 6). We find that the surface species giving rise to the upfield A_0 signal determines the pH dependence of the phosphate surface excess, while the surface excess of the phosphate associated with the downfield B_0 resonance is more or less constant in the pH range from 5.5 to 11.0 ($\Gamma^{Phosphate,downfield}$ = 0.27 ± 0.07 μmol m^{-2}). We could not include pH = 4 in this analysis because the signal is too broad to resolve the B_0 resonance.

The surface excess of the phosphate responsible for B_0 resonance would be equivalent to adsorbing ≈17 ± 4% of the total solution phosphate. Another way to visualize this result is to imagine that if the interstitial solution (which contains 0.1 mmol L^{-1} KDP) in the solids after

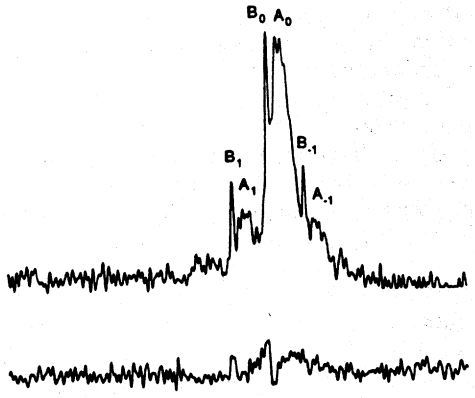

Figure 9. 121.49-MHz ^{31}P cross-polarization solid-state NMR spectra (85% H_3PO_4 external reference, scale in ppm): 256 scans, 256 data points zero-filled to 8k, 35.7-kHz spectral width, 5-s recycle time, 600-μs contact time. Freeze-dried boehmite with surface-adsorbed phosphate from a pH = 5.5 suspension, delay between spin-lock and acquisition: 1 μs (upper); 250 μs (lower). Main peaks are labeled with the subscript "0", first-ordering spinning side-bands with the subscript "±1".

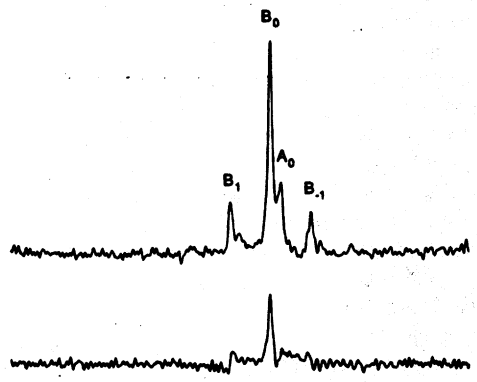

Figure 10. 121.49-MHz ^{31}P cross-polarization solid-state NMR spectra (85% H_3PO_4 external reference, scale in ppm): 256 scans, 256 data points zero-filled to 8k, 35.7-kHz spectral width, 5-s recycle time, 600-μs contact time. Freeze-dried boehmite with surface-adsorbed phosphate from a pH = 9.0 suspension, delay between spin-lock and acquisition: 1 μs (upper); 250 μs (lower). Main peaks are labeled with the subscript "0", first-order spinning side-bands with the subscript "±1".

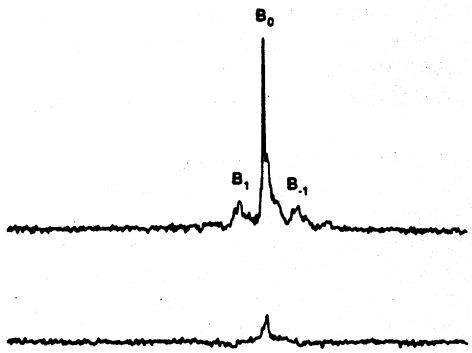

Figure 11. 121.49-MHz ^{31}P cross-polarization solid-state NMR spectra (85% H_3PO_4 external reference, scale in ppm): 256 scans, 400 data points zero-filled to 8k, 35.7-kHz spectral width, 5-s recycle time, 600-μs contact time. Freeze-dried boehmite with surface-adsorbed phosphate from a pH = 11.0 suspension, delay between spin-lock and acquisition: 1 μs (upper); 250 μs (lower). Main peaks are labeled with the subscript "0", first-order spinning side-bands with the subscript "±1".

centrifuging constituted 17 ± 4% of the total suspension volume (≈8.5 mL in our experiments since we used 50-mL suspension volumes), then freeze-drying the centrifugate would force the precipitation of this amount of interstitial-solution phosphate.

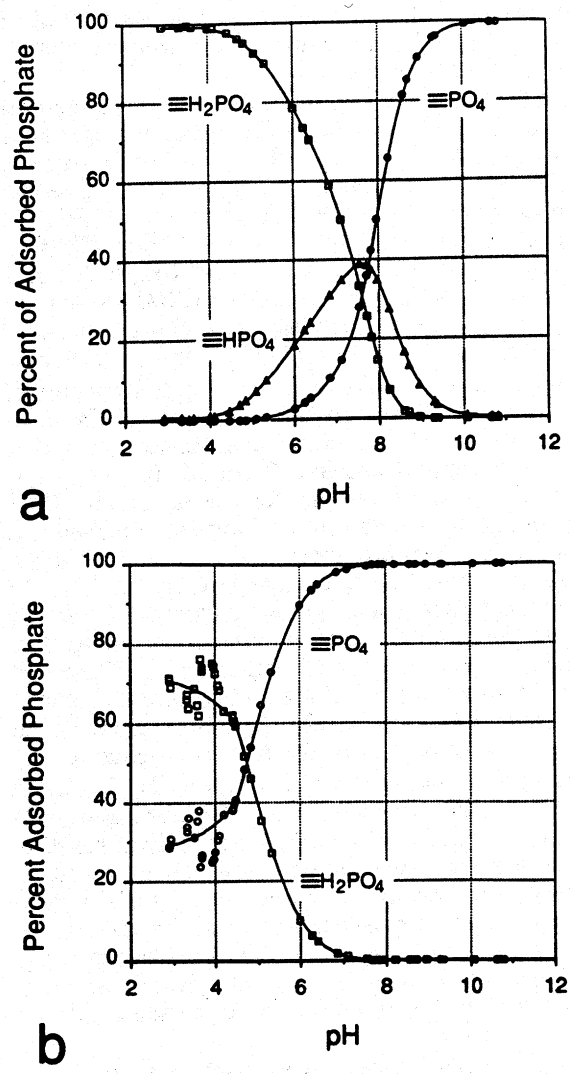

Figure 12. Surface speciation predicted from fitting the constant capacitance model to the titration and phosphate adsorption data appearing in Figures 1 and 4: (a) without aluminum phosphate solution complexes; (b) with aluminum phosphate solution complexes.

Discussion

1. Hydrolysis of Phosphate Surface Species. The phosphate surface speciation predicted by the constant-capacitance model using the average phosphate surface complexation constants for various aluminum oxides (log $K_{P^1(int)} = 9.34$, log $K_{P^2(int)} = 3.34$, log $K_{P^3(int)} = -2.87$) given by Goldberg and Sposito[54] is indicated in Figure 12a. The species $\equiv AlH_2PO_4^0{}_{(s)}$ dominates below pH = 7.5 and the species $\equiv AlPO_4^{2-}{}_{(s)}$ dominates above pH = 8. The species $\equiv AlHPO_4^-{}_{(s)}$ is of secondary significance since it never constitutes more than 40% of the phosphate surface excess. Phosphate speciation on the surface of boehmite predicted by the constant-capacitance model in the presence of aluminum–phosphate solution complexes is shown in Figure 12b. The model predicts that $\equiv AlH_2PO_4^0{}_{(s)}$ is the dominant phosphate surface species only up to pH = 4.5. At higher pH values, the nonprotonated species $\equiv AlPO_4^{2-}{}_{(s)}$ dominates.

We designed a series of ^{31}P solid-state NMR experiments to test in part the surface-speciation predictions made by the constant-capacitance model. We recognize that although surface-complexation models give the appearance of having a definite microscopic basis, Sposito[61] derived

(61) Sposito, G. *J. Colloid Interface Sci.* **1982**, *91*, 329.

a phenomenological model with the same mathematical structure. Still, this does not mean that speciation predictions are not valid.

Before discussing the NMR results, it would be helpful to translate the picture drawn by the constant-capacitance model into the language of NMR. Whether the surface speciation is as illustrated in Figure 12a (viz., some combination of all three species: $\equiv AlH_2PO_4^0{}_{(s)}$, $\equiv AlHPO_4^-{}_{(s)}$, and $\equiv AlPO_4^{2-}{}_{(s)}$) or as in Figure 12b (viz., a combination of only two species: $\equiv AlH_2PO_4^0{}_{(s)}$ and $\equiv AlPO_4^{2-}{}_{(s)}$), we would expect only one NMR resonance in the spectrum arising from these surface species because they are likely to be undergoing rapid chemical exchange.

Our reasoning is the following. ^{31}P NMR spectra of aqueous H_3PO_4–MOH solutions (M = Li, Na, K, Cs) show only one resonance because of chemical exchange involving the various phosphate species. If the lifetime of two or more species is short on the time scale of an NMR experiment, then a single peak will appear at a chemical shift that is the weighted average of the chemical shifts of those species undergoing chemical exchange. The pH dependence of this time-averaged resonance simply reflects changes in the proportions of the various species as they hydrolyze. In contrast, the two signals at ≈−8 and −10 ppm in ^{31}P solution spectra of Figure 5 represent chemical environments that are not in chemical exchange with one another on the time scale of the NMR experiment.

Surface species such as $\equiv AlH_2PO_4^0{}_{(s)}$, $\equiv AlHPO_4^-{}_{(s)}$, and $\equiv AlPO_4^{2-}{}_{(s)}$ differ only in the number of protons bound to the phosphate. Protons exchange rapidly in solution and, we would also expect, at an oxide/aqueous solution interface with the result that surface species of this type would be in rapid chemical exchange and give rise to only one resonance. Although our samples were freeze-dried, no effort was made to remove all water from them, and surface hydration would be sufficient to provide a pathway for proton exchange.

The appearance of more than one peak in the spectrum means that more than one chemical environment exists and these are not in rapid chemical exchange with one another. Arguing by analogy with the picture of phosphate chemical exchange in solution, these distinct chemical environments probably differ by more than simply the number of protons bound to the phosphate.

The speciation given in Figure 12a predicts that protonated phosphates would be significant as high as pH ≈ 9, while the speciation illustrated in Figure 12b predicts that protonated phosphates would be significant only as high as pH ≈ 6. "Dephased" CP-MAS results should indicate that pH at which this critical transition occurs.

Dipolar coupling between the ^{31}P nuclei of deprotonated surface phosphates and ^1H on the oxygens coordinating the aluminum atoms should still be sufficient to cross-polarize. In short, we should still expect to see a resonance in the CP-MAS spectra even when $\equiv AlPO_4^{2-}{}_{(s)}$ is the only surface species unless desorption of protons from the boehmite at high pH effectively strips the surface clean of protons.

Our results indicate that the pH dependence of the adsorption envelope is due primarily to a population of phosphates which we associated with the A_0 signal in our NMR spectra. The breadth and overall appearance of the A_0 signal suggests that it is generated by phosphate molecules existing in a range of chemical environments. A 7.0-T field strength is not sufficient to resolve distinct resonances in the A_0 signal.

This lack of resolution does not prevent us from drawing a number of valuable conclusions concerning the chemical environment of these phosphates. First, the chemical environment is directly influenced by the pH of the suspension. This comes as no surprise since we know that the surface charge and the affinity of the boehmite surface for adsorbing protons and hydroxyl ions is continuously changing with pH. Second, we interpret the "dephased" CP-MAS spectra (Figures 8–11) as proof the oxygens of those phosphates responsible for the A_0 signal are directly protonated. From this we conclude, there are still significant amounts of either $\equiv AlH_2PO_4^0{}_{(s)}$ or $\equiv AlHPO_4^-{}_{(s)}$ at pH = 9 and the transition to the point where $\equiv AlPO_4^{2-}{}_{(s)}$ dominates must occur between pH = 9 and pH = 11. Finally, desorption of protons from the surface of boehmite is sufficient to render ^1H–^{31}P cross-polarization impossible at pH = 11. ^1H–^{31}P cross-polarization does occur in wavellite where there are water molecules and hydroxyls coordinating aluminum atoms but none of the phosphate oxygens appear to receive hydrogen bonds.[60] Exactly how extensive deprotonation of the oxide surface must be in order to eliminate cross-polarization is not clear.

2. Surface Complexes and Surface Precipitates. An adsorbate may be in one of three major chemical environments at the mineral/aqueous solution interface: outer-sphere surface complexes, inner-sphere surface complexes, and surface precipitates. NMR experiments can provide very useful information about these chemical environments and their response to solution-pH changes. Hydrolysis in solution or at a mineral/solution interface represents a change in chemical environment observed as a pH-dependent chemical shift. Both inner- and outer-sphere surface complexes should exhibit pH-dependent chemical shifts (vide supra), distinguishing these chemical environments from surface precipitates.

The major property distinguishing inner- from outer-sphere surface complexes is their dynamics. Outer-sphere surface complexes are expected to display "solution-like" mobility, thereby averaging the principal components of the chemical-shift tensor. Spinning side bands would not be associated with solid-state NMR resonances of outer-sphere surface complexes. A rapidly tumbling outer-sphere complex would also be difficult to cross-polarize and may not appear in a CP spectrum.[62,63] An inner-sphere surface complex, on the hand, would most likely exhibit significant ssb intensity and ready cross-polarize. Thus, because the upfield A_0 signal displays ssb intensity and readily cross-polarizes, we conclude A_0 represents inner-sphere phosphate complexes with surface aluminum atoms.

Surface crystallites or precipitation nuclei could represent a chemical environment with the properties we observe for the narrow B_0 resonance. With the exception of certain crystalline materials synthesized by dissolving aluminum metal in phosphoric acid and the mineral taranakite,[62] there are no aluminum phosphates that we are aware of containing protonated phosphates in the crystal structure.[64] The B_0 resonance behaves as if it were not protonated yet in sufficiently close proximity to protons (possibly those in water molecules or hydroxyl ions coordinating the same aluminum to which the phosphate itself is bonded) to yield a resonance in a CP-MAS spectrum. The narrow peak width suggests a much more restricted chemical environment, while the intensity of the ssb supports the notion that the phosphates in this population are not motion averaged.

(62) Bleam, W. F.; Pfeffer, P. E.; Frye, J. S. *Phys. Chem. Miner.* **1989**, *16*, 809.
(63) Bank, S.; Bank, J. F.; Ellis, P. D. *J. Phys. Chem.* **1989**, *93*, 4847.
(64) Kniep, R. *Angew. Chem., Int. Ed. Engl.* **1986**, *25*, 525.

Such a crystallite would have to be small enough so that all phosphate anions in the nuclei would respond to changes in surface charge. The chemical environment at the surface is continuously changing with pH, as evidenced by the proton surface charge (Figure 1), the zeta potential of the suspension particles (Figure 2), and the chemical shift (Figure 8). Weiss et al.[65] observed a dependence of isotropic chemical shift on surface charge in the ^{29}Si NMR spectra of phyllosilicates. Though the surface charge in phyllosilicates arises from isomorphous substitution rather than protonation, it may be possible that the pH dependence of the ^{31}P chemical shift we are observing in the B_0 resonance arises from a variation of surface charge.

The phosphate surface excess on aluminum oxides at pH = 4 generally falls in the range of 2–3 μmol m^{-2}.[46,53,55] It would be fortuitous that these particular values would appear in at least three separate studies besides our own, unless a well-defined adsorption phenomenon were occurring. Phosphate removal from solution plateaued following repeated additions of phosphate in all of our "concentration null" experiments. If precipitation were occurring, we should not have seen a saturation of our adsorbing capacity through such an experiment. We conclude that we are, in fact, observing a well-defined adsorption phenomenon for which "surface-excess maxima" has meaning.

Until NMR spectra are collected on moist samples, the status of the B_0 resonance as a form of surface phosphate remains open. Our results are insufficient to conclusively rule out precipitation as an artifact of freeze-drying.

Conclusions

The properties of the broad A_0 signal confirm key elements of the hypothesis we were testing, viz. inner-sphere surface complexes form between phosphate and the aluminum atoms of the boehmite surface and the phosphates in these complexes hydrolyze with varying pH. Our results will not permit direct confirmation of the specific species that form, their stoichiometry, or the explicit form of binding.

The resolution of spectra from surface-adsorbed phosphate obtained by using the most advanced IR techniques, employing diffuse- and internal-reflectance cells and computer subtraction of background spectra, make detailed band assignments very difficult.[66,67] Yet, recently, Tejedor-Tejedor and Anderson[68,69] have presented evidence for the protonation of phosphate adsorbed on the surface of goethite.

Acknowledgment. We authors are grateful to Tom Boswell, Eastern Regional Research Center. W.F.B. wishes to thank summer interns Amy Saunders and Cliffae Wallace, who assisted with the adsorption experiments.

(65) Weiss, C. A.; Altaner, S. P.; Kirkpatrick, R. J. *Am. Mineral.* **1987**, *72*, 935.
(66) Nanzyo, M. *J. Soil Sci.* **1984**, *35*, 63.
(67) Nanzyo, M.; Watanabe, Y. *Soil Sci. Plant Nutr.* **1982**, *28*, 359.
(68) Tejedor-Tejedor, M. I.; Anderson, M. A. *Langmuir* **1986**, *2*, 203.
(69) Tejedor-Tejedor, M. I.; Anderson, M. A. *Langmuir* **1990**, *6*, 602.